Achievable accuracy in brain tumors by *in vivo* dosimetry with diode detectors

M. Allahverdi[1*] and M.R. Taghizadeh[2]

[1] Department of Medical Physics, Cancer Institute, Tehran University of Medical Sciences, Tehran, Iran
[2] Department of radiotherapy, Imam Khomeini Hospital, Tehran University of Medical Sciences, Tehran, Iran

Background: *In vivo* measurements of applied dose during radiotherapy treatment, is important to ensure accurate dose delivery to patients. Uncertainty in dose delivery should fall within ±5% of the prescribed dose as recommended by ICRU. Assessment of dose for radiotherapy applications performed with various types of detectors. In this study, semiconductor diodes were used which have some advantages for clinical dosimetry. ***Materials and Methods:*** The brain tumors have generally treated with two fields using SSD technique. Entrance and exit dose were measured for each patient with diodes during treatment. Entrance and exit dose measurements have converted to midline dose. Measured entrance and exit doses have compared with calculated ones and large deviations (more than 5%) have observed. A farmer ionization chamber (0.6 cm) was used as the reference dose detector and a Perspex water phantom (30¤30cm² area and thickness ranging from 5 cm to 30 cm) were used to determine calibration and correction factors. ***Results:*** Correction factors were determined and variations more than 1% have used to obtain correct doses. Large deviations between measured and calculated for entrance (5.3%), exit (42%) and midline (47%) were detected. The difference was not found to be significant when comparing the measured entrance dose with the calculated one (p=0.696) and the measured exit dose with calculated one (p=0.643) and measured midline dose with calculated one (p=0.104). ***Conclusion:*** *In vivo* dosimetry is very useful to check the dose delivered to the patient. A high precision obtained when the calibration and correction factors for each parameter of influence on the diode response are carefully determined and applied to convert the diode signal in the adsorbed dose. In this study, the target-absorbed doses were estimated from the measured entrance dose and the measured transmission. **Iran. J. Radiat. Res., 2006; 3 (4): 153-161**

Keywords: *In vivo dosimetry, brain tumors, semiconductor detectors.*

INTRODUCTION

During radiotherapy, high accuracy in dose delivery is required because the relationships between absorbed dose and local tumor control and particularly normal tissue damage are very steep. In many institutions, *in vivo* dosimetry using diodes and TLDs is performed to check the actual dose delivery[1-6]. The ideal diode for *in vivo* should show small dependence (less than %1) on the field size, source-skin distance (SSD), interposition of modifying devices such as wedges, trays, partial transmission blocks and orientation of beam. Moreover, correction factors have modified with accumulated dose. The loss of sensitivity with the accumulated dose should be kept as low as possible. All these requirements must be fulfilled taking into consideration that the field perturbation caused by the diode should be minimal[7]. The aim of this work was to study the dosimetric characteristics of p-type diode designed to cover the ^{60}Co beam for *in vivo* dosimetry and the method of dose evaluation in patients irradiated by ^{60}Co beam. Understanding the characteristics of the diode to be used in clinical routine is important, because the correction factors that have to be applied to the reading of diode to give real dose differ a lot from type to type[5]. An important aspect of a quality assurance program is a check on the actual doses delivered to the patients. Uncertainty in dose delivery should in general, fall within ±5% of the prescribed dose as recommended by the International Commission on Radiation Units and Measurements (ICRU) [8].

MATERIALS AND METHODS

Materials

In vivo detectors used in this study were

*Corresponding author:
Dr. Mahmoud Allahverdi, Department of Medical Physics, Tehran University of Medical Sciences, Tehran, Iran
Fax: *+98 21 66482654*
E-mail: *malahverdi@yahoo.co.uk*

T60010L P-type semiconductor diodes with a build-up cup of titanium (Total build-up=1.0 g/cm²) adequate for 1-5 MV photon energies and were connected to a MULTIDOS electrometer (T10004). A farmer TM30010 Ionization chamber (0.6 cm) connected to a UNIDOS electrometer (T10001) was used as the reference dose detector. All devices are from PTW Freiburg, Germany. A Perspex water phantom (30×30 cm² area and thickness ranging from 5 cm to 30 cm) was used to determine calibration and correction factors. This phantom has a special slab to accommodate the ionization chamber.

Methods

The diodes were subjected to a set of tests that we initially performed because these diodes had been received newly. These initial tests consist of the measurement of:

a) **Signal stability after irradiation:** The display of the signal taken immediately after irradiation was compared with the display of the signal 5 min after the end of irradiation[5].

b) **Intrinsic precision:** the mean and the standard deviation of ten measures were calculated[5].

c) **Antero-posterior symmetry:** the ratio of the diode reading when irradiated with its round side facing the collimator, and when irradiated with its flat side facing the collimator, is obtained. To fix the diode with its round build-up cap on the phantom the special slab in which the diode could be inserted was used. The diode measuring point was considered to be on its round side[5].

d) **Dose decrease under the diode:** the dose decrease at 5 cm depth under the diodes was measured in Perspex water phantom using a small volume ionization chamber (TM31014)[5, 9, 10].

Calibration procedure

When initial tests were performed, the diodes were calibrated to measure the entrance dose, D_{en}, and the exit dose, D_{ex}. On the other hand, when silicon diodes are used, many parameters have to be taken into consideration[2]. In order to calibration of the silicon diodes, the procedure reported by Rizzotti *et al.* was followed[1]. The phantom was placed on the treatment couch and the gantry was rotated to 90 degrees. The calibration was performed with the diodes positioned on the entrance and exit surfaces of a Perspex water phantom (30×30 cm² area and 5-30 cm thickness), with 15 cm thickness at the center of a 10×10 cm² field size. Then, the ion chamber was inserted into the water phantom of 25°C at depth d_{max} from the entrance and exit surfaces to calibrate these detectors in terms of entrance and exit doses. ⁶⁰Co γ-rays were used at SSD of 80 cm with a 90°- gantry angle.

Such calibrations were performed in two parts: the calibration in reference set-up conditions to establish the detector calibration factors for absorbed dose to water and the establishment of correction factors to account for the differences in various experimental conditions. The symmetrical definitions of D_{en} and D_{ex}, defined at points along the beam axis at depth d_{max} below the entrance and exit surfaces, were a convenient and simple procedure for two opposed beams in the derivation of the midline dose, D_{mid}[1, 11, 12]. In actual measurements, the placement of detector on the entrance surface was made by a slight shift from the beam axis to avoid the shadow effect [6].

The calibration factor (F) was then determined as ratio of the adsorbed dose measured with the ionization chamber, D, and the reading of the diode, M; in reference conditions (figure 1).

$$F = \left(\frac{D}{M} \right)$$
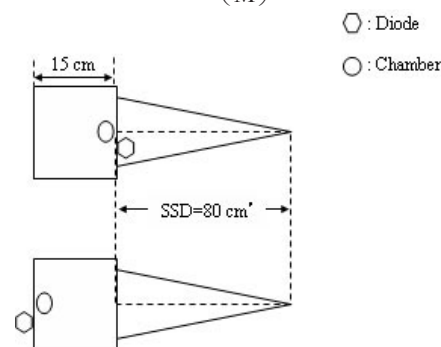
Figure 1. Determination of the entrance and exit calibration factors for diodes. The diodes were calibrated in reference condition: 80 cm SSD, 10×10 cm field size, temperature=25 C, gantry angle=90 , 15 cm Perspex water phantom.

Correction factors

As earlier mentioned, the calibrations were performed at the reference set-up conditions (Thickness=15 cm, 80 cm source-surface distance (SSD), field size = 10⋈10 cm² on the surface, temperature = 25°C, gantry angle = 90° and no wedge). Correction factors were required to account for the calibration differences when measurements were performed under various experimental conditions [10, 11, 13, 14]. For instance, correction factors were established for the different source-surface distance (SSD), field size, thickness and the irradiation angles. The entrance and exit correction factors © were defined as:

$$C = \frac{(D/M)_{mes}}{(D/M)_{ref}}$$

$(D/R)_{mes}$: The ratio of the entrance or exit dose and the relevant entrance or exit diode signal were measured in geometry of interest.

$(D/R)_{ref}$: The ratio of the entrance or exit dose and the relevant entrance or exit diode signal were measured in reference condition.

Complete backscatter

The exit dose was not measured in complete backscatter conditions. Backscatter factor has to be taken into account to compensate for the full backscatter loss for exit doses measured with diodes. A backscatter correction factor (B') was determined as the ratio of the ionization chamber reading in full backscatter conditions (R_{FB}) and ionization chamber reading in exit dose measurement condition (R_{MC}) for different field size [11,15].

$$B' = \frac{R_{FB}}{R_{MC}}$$

Dependence of diode response on temperature

The diodes may show sensitivity variation for temperature [16]. A thermostat equipped Perspex tank, filled with water, was used with ^{60}Co unit. In order to simulate real clinical conditions, diodes were taped on the tank surface; the temperature of water in the tank was measured with a digital thermometer with a sensitive sensor. The tank surface temperature was increased slowly from 22°C to 32°C (average skin temperature). The sensitivity of the diodes was determined at different temperatures and expressed relatively to that at 25°C. The diodes were placed on the surface of the tank more than 10 min in order to allow the diodes to reach full thermal equilibrium with thank surface.

Entrance and exit dose

The entrance and exit doses [6, 11, 15] are given by: $D_{en} = M_{en} \cdot F_{en} \cdot |P|_i \ C_i^{ex}$ and $D_{ex} = M_{en} \cdot F_{ex} \cdot |P|_i \ C_i^{ex}$.

Where C_i^{en} and C_i^{ex} are the entrance correction factors and the exit correction factors for different conditions.

Shadow effect of entrance diode

To avoid the shadow effect, either the entrance detector or the exit detectors should be shifted slightly off the beam axis. Since the exit dose is more sensitive to the position displacement, it recommended that to keep the exit detector on the axis and shift the entrance detector off the axis.

Determination of transmission

For our purpose, it was better to determine the exit transmission, T_{ex} , and the midline transmission, T_{mid} [1,11]. The exit transmission, T_{ex} , was calculated from the ratio of the dose at exit and entrance depths, which are separated by a thickness of (z-1) cm of water equivalent tissues, z, represents the total water equivalent thickness (figure 1):

$$T_{ex} = \frac{D_{ex}}{D_{en}}$$

The midline transmission, T_{mid} , was calculated from the ratio of the dose at midline depth (z/2) and entrance depth:

$$T_{mid} = \frac{D_{mid}}{D_{en}}$$

At the beginning, a set of data on T and T were established in phantom measurements of different phantom thicknesses. Transmission curves for T_{ex} and T_{mid} as a function of water

equivalent thickness were then determined. For clinical applications of in vivo dosimetry, the midline dose was determined from measured entrance and exit doses of the patient using these transmission curves: $D_{mid} = D_{M,en} \times T_{mid}$

In this study, the midline dose (D_{mid}) delivered to the patient was estimated from *in vivo* measurements as explained and compared to the expected midline dose ($D_{cal,mid}$) calculated manually. Although the water equivalent thickness is measured in a phantom, it represented an expansion or compression of the real patient to a water equivalent patient. Such an expansion or compression is useful if tissue inhomogeneities are symmetrical with respect to the midline position. For tissues irradiated in the head and neck fields, the symmetrical disposition of the tissues guarantees the method of midline target dose determination.

RESULTS

Initial tests

The diode tests results are shown in table 1.

Table 1. Results of the initial tests performed on the diodes.

	T60010L-142	T60010L-143
Stability after irradiation (After 5 min.)	0%	0%
Intrinsic precision (SD) (10 irradiation)	0.07%	0.09%
Front-back symmetry (ratio)	1.28	1.29
Dose decrease (under the diode) at 5 cm depth	4%	4%

Calibration factor

The entrance calibration factors for T60010L-142 and for T60010L-143 are 3.7 and 3.76, and the exit calibration factor for T60010L-142 and for T60010L-143 are 5.4 and 5.28, respectively.

Correction factors
Field size correction factor

The effect of field size on diode response was obtained for two diodes. One T60010L-142 was used for entrance and the other T60010L-143 used for exit field size correction factor.

Entrance field size correction factor ($C_{f.s.}^{en}$)

Entrance field size correction factor of diode is shown in figure 2. As seen, it has a correction factor greater than 1% for field sizes 5×5 cm² and 6×6 cm² , but it has negligible correction factor less than 1% for field sizes above 6×6 cm² .

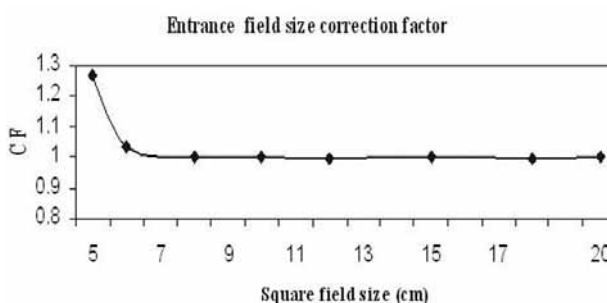Figure 2. Entrance field size correction factor as a function of field size.condition: 80 cm SSD, 10×10 cm field size,temperature=25 C, gantry angle=90 , 15 cm Perspex water phantom.

Exit field size correction factor ($CF_{f.s.}^{ex}$) :

Exit field size correction factor of diode is shown in fig. 3. As can be seen, it has a correction factor greater than 1% for field sizes 5×5 cm² , 6×6 cm² and 8×8 cm² , but it has negligible correction factor less than 1% for field sizes above 8×8 cm² .
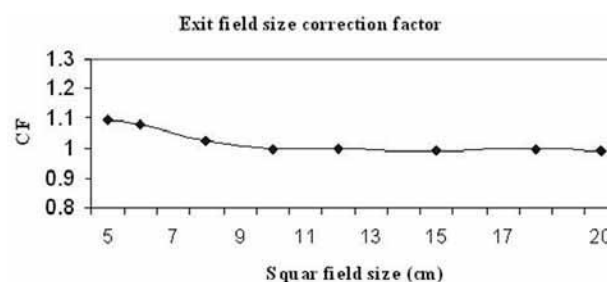

Figure 3. Exit field size correction factor as a function of field size.phantom.

SSD correction factor

SSD correction factors were obtained for two diodes. One T60010L-142 was used for

entrance and the other T60010L-143 used for exit SSD correction factor.

Entrance SSD correction factor (C_{SSD}^{en})

Figure 4 shows the variation of C_{SSD}^{en} for entrance diode. C_{SSD}^{en} increases about 3% when increasing the SSD from 60 to 80 cm and increases about 1.2 % when the SSD increases from 80 to 95 cm.
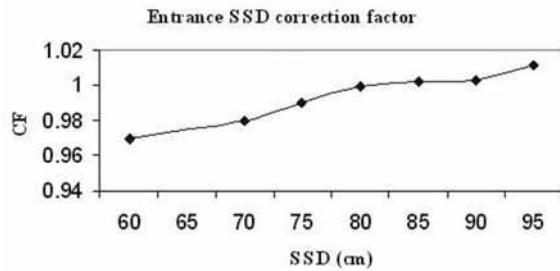

Figure 4. SSD correction factor as a function of SSD.

Exit SSD correction factor (C_{SSD}^{ex})

Figure 5 shows the variation of C_{SSD}^{ex} for exit diode. C_{SSD}^{ex} decreases about 6.4% when increasing the SSD from 60 to 95 cm.
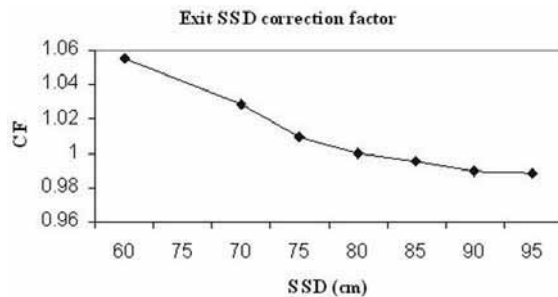

Figure 5. Exit SSD correction factor for as a function of SSD.phantom.

Thickness correction factor (C_z)

Figure 6 shows the variation of (C_z) for exit diode. C_z increases more than 1% when increasing the thickness from 5 to 15 and C_z increases more than 1% when increasing the thickness from 15 to 20 cm, so thickness correction factor decreases more than 1%.
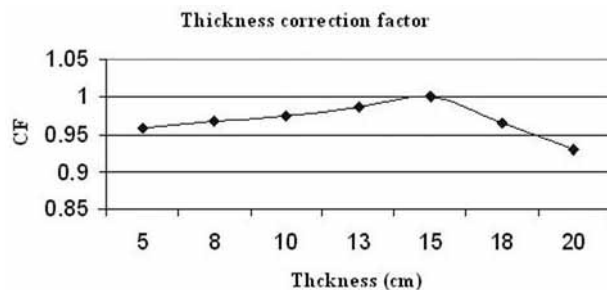

Figure 6. Thickness correction factor for as a function of thickness.

Directional response

Figure 7 shows the dependence of diode for different angle between the central beam axis and the symmetry axis of the diode. Directional response of diode from 0°to 70°and in opposite direction from - 70°to 0° is about 0.45% and 0.63%, respectively.
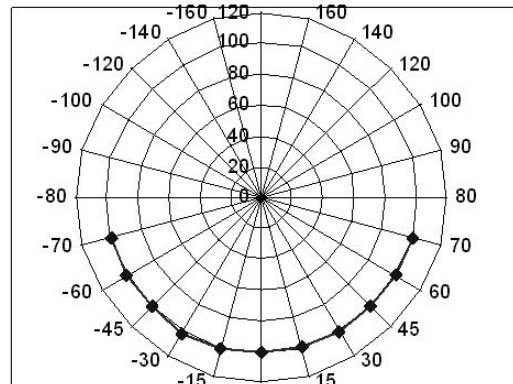

Figure 7. The sensitivity of diode as a function angle between the central beam axis and the symmetry axis.

Temperature dependence

The effect of temperature on each diode's response is shown in figure 8. A linear increase of the diode signal with temperature is found.
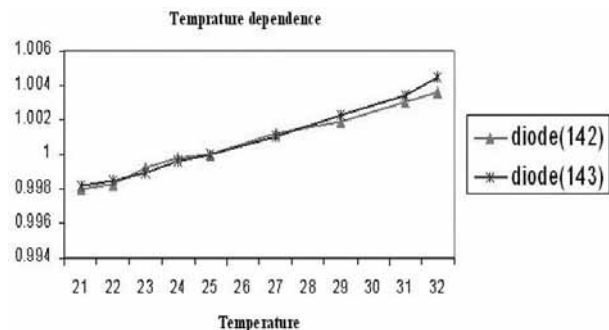

Figure 8. Sensitivity dependence on temperature for both diodes.

Shadow effect of entrance diode

Figure 9 shows a plot of the relative response by the exit diode as a function of entrance diode displacement. It is seen that full recovery in the response occurs, as the displacement is more than 1 cm. Therefore, the shift of entrance diode by 2 cm off the beam axis was adopted.

Complete backscatter

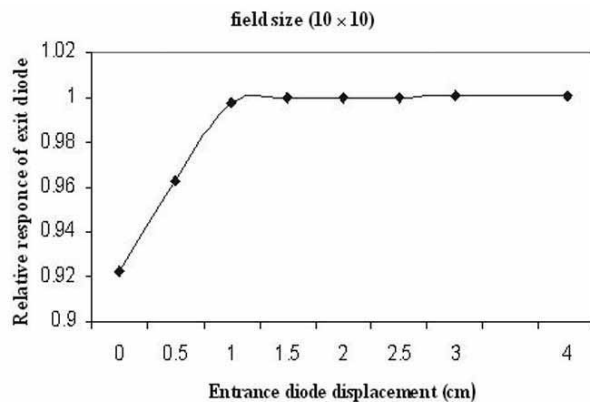A backscatter correction factor (B⁄) was determined as the ratio of the ionization

Figure 9. The results of phantom measurements in reference conditions for the relative response of exit diode as a function of entrance diode displacement from the beam axis.

chamber reading in full backscatter conditions (R_{FB}) and ionization chamber reading in exit dose measurement condition (R_{MC}) for different field size (figure 10).
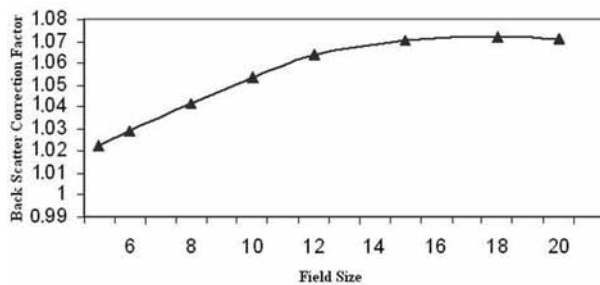

Figure 10. Backscatter correction factor. The backscatter correction factor is plotted as a function of the field size. thickness.

Determination of transmission

Transmission curves for T_{ex} and T_{mid} as a function of water equivalent thickness were determined (figure 11). The curves shown in figure 11 have been derived at 80 cm SSD.
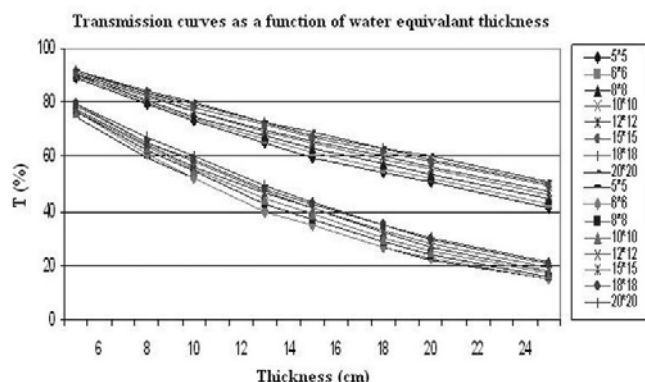

Figure 11. Transmission curves for T and T as a function of water equivalent thickness. T curves are up and T curves are down.

Treatment accuracy

Combined entrance and exit dose measurements have been performed on 38 patients treated for brain tumors. All these patients were treated with SSD set-up by ^{60}Co. The *in vivo* measurements discussed in this study are entrance and exit dose measurements performed on the lateral treatment fields. The results of the entrance dose measurements, exit dose measurements, midline dose determinations and transmission measurements are plotted in histograms as deviation from calculated dose (%). The negative deviation, defined as ($(D_{mes}-D_{cal})/D_{cal}\times100$), indicates that measured doses are lower than calculated doses.

Entrance dose measurement

The results of the ($(D_{M,en}-D_{cal,en})/D_{cal,en})\times100$) show a Gaussian distribution with mean value of -0.2% and the standard deviation of 3.04% (figure 12). A large error has been defined as discrepancy between measured and calculated dose larger than 5%. Such errors have been detected in 5.3% (2/38) of measured treatment set-ups. The difference were not found to be significant (P=0.696) when comparing measured entrance dose with calculated entrance dose.
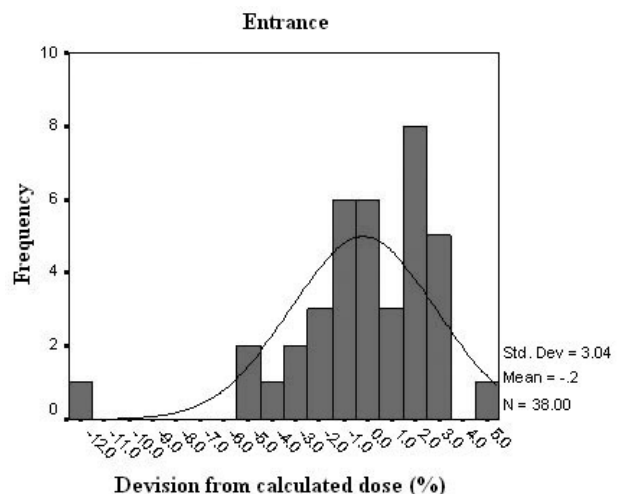

Figure 12. The relative deviation of measured entrance doses from calculated entrance doses as percentage for the treatments of brain tumor.

Exit dose measurement

The results of the ($(D_{M,ex}-D_{cal,ex})/D_{cal,ex})\times100$) show a Gaussian distribution with mean

value of -1.6% and the standard deviation of 6.99% (figure 13). Large errors have been detected in 42% (16/38) of measured treatment set-ups. The difference were not found to be significant (P=0.643) when comparing measured exit dose with calculated exit dose.
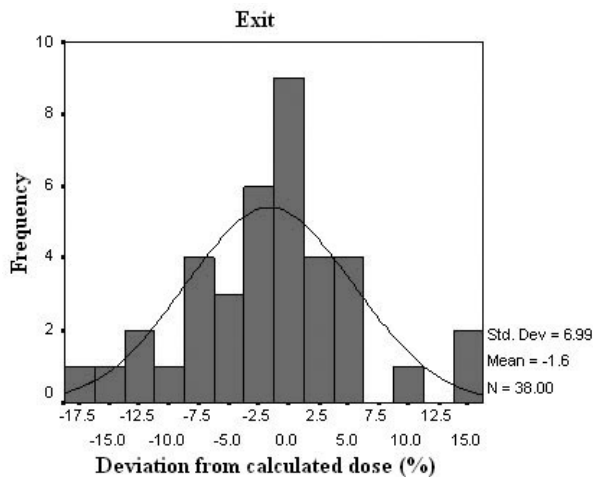

Figure 13. Transmission curves for T and T as a function of water equivalent thickness. T curves are up and T curves are down.

Transmission measurements

The results of the $((T_M-T_{cal})/T_{cal})$ as percentage are plotted in figure 14. A broad distribution is found with a mean value of -1.3% and standard deviation of 7.52%. Large deviations of the T_M from T_{cal} have been detected in 39.4% (15/38) of treatment set-ups measured.
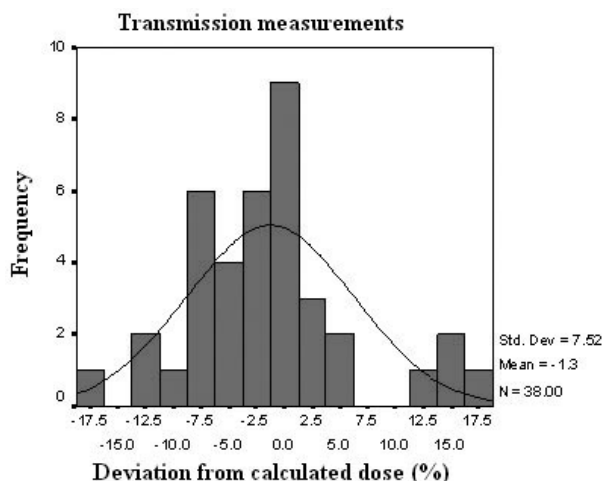

Figure 14. The relative deviation of transmission measurements from calculated transmission measurements as percentage.

Midline dose measurement

In figure 15, the frequency distribution of the percentage ratios of ((measured midline dose - calculated midline dose)/ calculated midline dose)) show a Gaussian distribution. The mean value is -5.5% and the standard deviation of 4.32%. Large errors have been detected in 47% (18/38) of the treatment set-ups measured. The difference were not found to be significant (P=0.104).
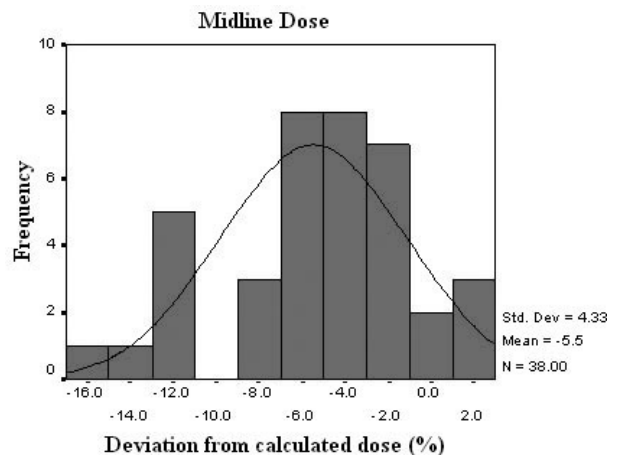

Figure 15. Absorbed midline dose (D_{mid}) as percentage value of the calculated midline dose ($D_{cal,mid}$) treatments of brain tumor.

DISCUSSION

Initial tests showed that both diodes had excellent signal stability, 5 minutes after irradiation, and an acceptable intrinsic precision. In order to obtain correct doses, calibration factors were used to calculate entrance and exit dose in reference and non-reference conditions. Correction factors with variation about 1% were used. The effect of direction responses was ignored due to the fact that all of the measurements had been done at perpendicular position in zero degree. The effect of temperature on diodes was ignored because of small variation of temperature in treatment room. For removing the shadow effect, entrance diode was placed 2 cm off the center axis.

As mentioned before, the exit was measured in lack of backscatter conditions, so for converting the measured exit dose to complete conditions, complete backscatter was used. As it was observed, with increasing

the field size the need for this factor increases (figure 10).

After calculating entrance and exit doses and transmission measurement, large errors were checked. Statistical examinations showed that differences were not significant, when measured doses were compared with calculated doses.

Comparison between figures 14 and 12 showed a broader distribution for $(T_M - T_{cal})/T_{cal})$ percentage values than $(D_{M,en} - D_{cal,en})/D_{cal,en})$ percentage values (SD=7.52% against SD=3.04%).

This was expected, because the transmission measurement T_M depends on patient-related uncertainties such as contour errors (error on thickness), and tissue inhomogeneities (type of tissues) which have no or only a small influence on the entrance dose $(D_{M,en})$.

Large errors detected in midline dose measurement, when comparing measured midline dose with calculated midline dose. Although there are a number of reasons responsible for such deviations, an apparent contribution is the inhomogeneities.

Figure 16 shows the relative deviation of measured water equivalent thicknesses from recorded geometric thicknesses. The positive deviation, defined as ((water equivalent thickness - recorded geometric thickness)/ recorded geometric thicknesses)), for most fields indicates that measured water equivalent thicknesses are larger than recorded geometric thicknesses. In most cases, a strong correlation between deviations in
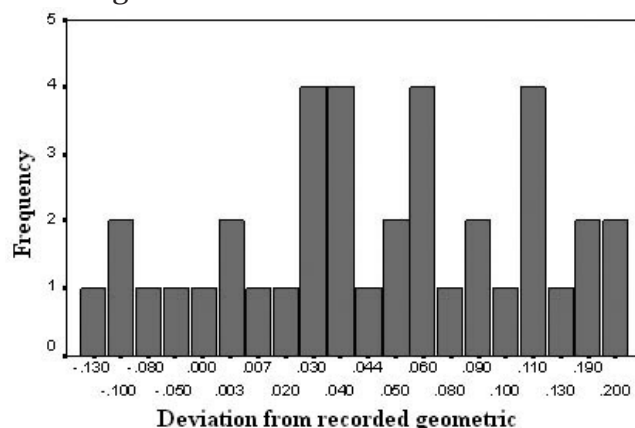

Figure 16. Relative deviation of measured water equivalent thickness from recorded geometric thicknesses.

dose and body thickness is evident.

CONCLUSION

In vivo measurements have been proved to be a very useful as check for the dose delivered to a given patient. A high precision can be obtained when the calibration and correction factors for each parameter of influence on the diode response are carefully determined and applied to convert the diode signal in adsorbed dose. The exit dose measurements with diode detectors can be performed and are reliable when due correction factors are determined and applied for exit dose measurement conditions, e.g. correction for lack of backscatter. Much care has to be taken for the correct positioning of the diodes to avoid shadowing effect. The main advantage of using diode detectors for *in vivo* dosimetry is that results are available in real time. Diode *in vivo* dosimetry is also less time consuming as compared to TLD *in vivo* dosimetry; however, the target absorbed dose or the dose delivered to critical organs is more important than the entrance or exit dose.

In this study, the target-absorbed doses were estimated from the measured entrance dose and the measured transmission. Initially the study of this method (determination of calibration factors, correction factors, determinations of the curves of T_{ex} and T_{mid}) is difficult and time consuming, but entrance and exit doses can easily be measured with placing diodes on the entrance and exit surface of the skin. Comparing measured entrance, exit and midline doses with due calculated doses, errors can be detected if the difference between measured and calculated is more than 5%.

Some of the sources of errors are Inaccuracies in algorithm, errors in set-up, patient motion, errors on contours determination, tissue inhomogeneities, and error in placing diodes. In this study, errors in the entrance doses are less than the doses in midline points and in the exit, doses are more than the midline doses. In most cases, a correlation between deviations in dose and body

thickness is evident. If the target doses were calculated using patient geometric thickness, the mean value and the standard deviation were -5.5% and 4.32%, respectively. If the target doses were calculated using patient water equivalent thickness, the mean value will increase and the standard deviation will decrease [6]. Finally, in vivo dosimetry is a useful method for quality control in radiotherapy and increasing treatment accuracy

REFERENCES

1. Rizzotti A, Compri C, Garusi GF (1985) Dose evaluation to patients irradiated by ^{60}Co beams, by means of direct measurement on the incident and on the exit surfaces. *Radiother Oncol, 3: 279-283.*

2. Nilsson B, Ruden BI, Sorcini B (1988) Characteristics of silicon diodes as patient dosimeters in external radiation therapy. *Radiother Oncol 11: 279-288.*

3. Leunens G, Van Dam J, Dutreix A ,Van der Schueren, E (1990) Quality assurance in radiotherapy by *in vivo* dosimetry. 2. Determination of the target absorbed dose. *Radiother Oncol, 19: 73-87.*

4. Alecu R, Loomis T, Alecu J, Ochran T (1999) Guidelines on the implementation of diode *in vivo* dosimetry programs for photon and electron external beam therapy. *Med Phys, 24: 5-12.*

5. Jornet N, Ribas M, Eudaldo T (2000) *In vivo* dosimetry: Intercomparision between p-type based and n-type based diodes for the 16-25 MV energy range. *Med Phys, 27: 1287-1293.*

6. Tung CJ, Wang HC, Lo HS, Wu JM , Wang CJ (2004) *In vivo* dosimetry for external photon treatments of head and neck cancers by diodes and TLDs. *Radiation Protection Dosimetry, 111: 45-50.*

7. Alecu R, Feldmeier JJ, Alecu M (1997) Dose perturbations due to *in vivo* dosimetry with diodes. *Radiother Oncol, 42: 289-291.*

8. International Commission on Radiation Units and Measurements (1976) Determination of absorbed dose in patients irradiated by beams of X and gamma rays in radiotherapy procedures. ICRU Report 24 Washington DC. *45-62.*

9. Meigooni AS, Sowards K, Myron G (2002) Evaluation of the veridose *in vivo* dosimetry system. *Medical Dosimetr, 27: 29-36.*

10. Ehringfeld C, Schmid S, Poljanc K, Kirisits C, Aiginger H, Georg D (2005) Application of commercial MOSFET detectors for *in vivo* dosimetry in the therapeutic X-ray range from 80 kV to 250 kV. *Phys Med Biol, 50: 289-303.*

11. Leunens G, Van Dam J, Dutreix A , Van der Schueren, E (1990) Quality assurance in radiotherapy by *in vivo* dosimetry. 1. Entrance dose measurements, a reliable procedure. *Radiother Oncol, 17: 141-151.*

12. Huyskens D, Van Dam J, Dutreix A (1994) Midline dose determination using *in vivo* dose measurements in combination with portal imaging. *Phys Med Biol, 39: 1089-1101.*

13. Heukelom S, Lanson JH, Mijnheer BJ (1992) *In vivo* dosimetry during pelvic treatment. *Radiother Oncol, 25: 111-120.*

14. Millwater CJ, Macleod AS , Thwaites DI (1998) *In vivo* semiconductor dosimetry as part of routine quality assurance. *British Journal of radiology, 71: 661-668.*

15. Cozzi L and Fogliata-cozzi A (1998) Quality assurance in radiation oncology. A study of feasibility and impact on action levels of an *in vivo* dosimetry program during breast cancer irradiation. *Radiother Oncol, 47: 29-36.*

16. Grusell E and Rikner G (1986) Evaluation of temperature effect in p-type silicon detectors. *Phys Med Biol, 31: 527-534.*